Plant Physiology and Biochemistry 142 (2019) 84–93

Contents lists available at ScienceDirect

Plant Physiology and Biochemistry

journal homepage: www.elsevier.com/locate/plaphy

Research article

Identifying S-nitrosylated proteins and unraveling S-nitrosoglutathione reductase-modulated sodic alkaline stress tolerance in *Solanum lycopersicum* L

Biao Gong[a,b], Qinghua Shi[a,b,*]

[a] State Key Laboratory of Crop Biology, Shandong Agricultural University, Taian 271018, PR China
[b] Collaborative Innovation Center of Fruit & Vegetable Quality and Efficient Production in Shandong, Key Laboratory of Biology and Genetic Improvement of Horticultural Crops in Huanghuai Region, Ministry of Agriculture and Rural Affairs, PR China

ARTICLE INFO

Keywords:
GSNOR
RNS
S-nitrosylation
Sodic alkaline stress
Tomato

ABSTRACT

S-nitrosylation, regulated by S-nitrosoglutathione reductase (*GSNOR*), is considered as an important route for nitric oxide (NO)-modulated stress tolerance in plants. However, genetic evidence for the *GSNOR*-mediated integrated regulation of S-nitrosylation and plant stress response remains elusive until now. In the present study, we used a site-specific nitrosoproteomic approach to identify 334 endogenously S-nitrosylated proteins with 425 S-nitrosylated sites from the wild type (WT) and *GSNOR*-knockdown (G) tomato plants under both control (C) and sodic alkaline stress (S) conditions. In detail, the results revealed 68, 92, 54 and 56 up-regulated, as well as 10, 36, 14 and 10 down-regulated S-nitrosylated proteins in G-C/WT-C, G-S/WT-S, WT-S/WT-C, and G-S/G-C, which is the first dataset for S-nitrosylated proteins in *Solanaceae*. These S-nitrosylated proteins are involved in a wide range of various metabolic, cellular and catalytic processes. Based on this data, proteins involving in NO homeostasis control, signaling of Ca^{2+}, ethylene and MAPK, reactive oxygen species (ROS) scavenging, osmotic regulation, as well as energy support pathway have been identified and selected as the key and sensitive targets that were regulated by *GSNOR*-modulated S-nitrosylation in response to sodic alkaline stress. Taken together, *GSNOR* is actively involved in the regulation of sodic alkaline stress tolerance by S-nitrosylation. And the present study provided valuable resources and new clues for the study of S-nitrosylation-regulated metabolism in tomato plants.

1. Introduction

Sodic alkaline stress, which is defined as the existence of alkaline salts mainly including $NaHCO_3$ and Na_2CO_3 in soil (Gong et al., 2013), is one of the most crucial abiotic stressors which plants encounter in the era of climate change. Large numbers of studies have indicated that sodic alkaline stress is more hazardous than saline stress to plant growth and development, owing to the additional high pH stress (Gong et al., 2013, 2014a and 2014b). High pH stress usually leads to reduction in the nutrient availability of P, K, Ca, Mg, Fe and Zn in soil, destruction of cellular or subcellular structure, deterioration of normal root function, disorder in nutrient uptake and assimilation, and thus resulting in a significant decrease in plant growth vigour as well as yield of agricultural crops (Gong et al., 2014c; Cellini et al., 2011.). Excepting saline stress induced physiological drought and ion toxicity, plants in sodic alkaline stress must cope with intracellular as well as rhizospheric high pH conditions.

Nitric oxide (NO) is a hydrophobic, highly diffusible gaseous molecule with a broad spectrum of regulatory functions involved in various plant growth, developmental processes, as well as stress response (Sami et al., 2018). In plant cell, S-nitrosoglutathione (GSNO) is a major biologically active form of reactive nitrogen species (RNS) and functions as a primary nitrosothiol donor (Leterrier et al., 2011). In addition, NO can react with reduced glutathione (GSH) to form S-nitrosoglutathione (GSNO), which also can be spontaneously broken down into NO and GSH, or be specifically reduced by S-nitrosoglutathione reductase (GSNOR) to glutathione disulfide (GSSG) and NH_3 (Zhan et al., 2018). Thus, GSNO plays roles of both NO pool and donor, which can be sensitively regulated by GSNOR. So, functions of *GSNOR* in maintaining intracellular homeostasis of GSNO and NO, have aroused great interest in recent years (Feechan et al., 2005; Begar-Morales et al., 2014; Gong et al., 2015; Saxena et al., 2018; Zhan et al., 2018).

As a general rule, activities of proteins are mediated by dedicated

* Corresponding author. State Key Laboratory of Crop Biology, Shandong Agricultural University, Taian 271018, PR China.
E-mail address: qhshi@sdau.edu.cn (Q. Shi).

https://doi.org/10.1016/j.plaphy.2019.06.020
Received 14 January 2019; Received in revised form 13 June 2019; Accepted 13 June 2019
Available online 15 June 2019

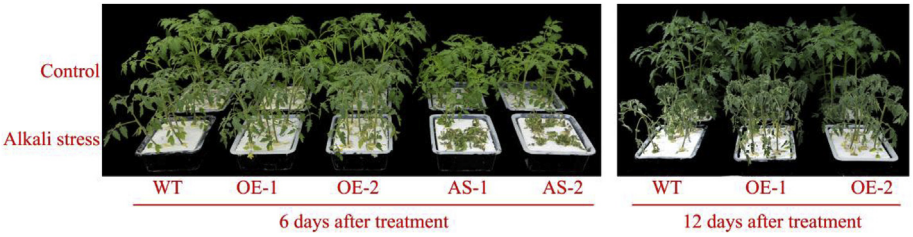

Fig. 1. Photographs of wild type (WT) seedlings and transgenic seedlings (OE means *GSNOR* overexpression seedlings; AS means *GSNOR* knock down seedlings) were taken 6 and 12 d after treatment. This figure was cited from Fig. 3A of Gong et al. (2015).

enzymatic mechanisms including a panoply of function-regulating post-translational modifications (Seth et al., 2018). For one of the common reversible posttranslational modification, an NO molecule can be covalently added onto Cys thiol to form S-nitrosothiol. This process is named protein S-nitrosylation and acted as a major physiological effect of NO in cellular functions (Wolhuter et al., 2018). Protein S-nitrosothiols are highly sensitive mechanism in response to the intracellular redox status, especially RNS homeostasis, to regulate the cellular signaling (Rizza et al., 2018). A growing numbers of evidence indicate that there are various protein S-nitrosylation regulated mechanisms involving enzymatic activity, three-dimensional conformation changes, stability, subcellular localization, ligand binding and protein-protein interaction (Gusarov et al., 2018). Until now, there are some numbers of reports related to protein S-nitrosylation mechanism in plant system (Malik et al., 2011). However, little information can be found about the protein S-nitrosylation mechanism in tomato (*Solanum lycopersicum* L.) plants.

In *Arabidopsis*, protein S-nitrosylation has been confirmed as a key mechanism in NO-modulated stress tolerance. RNS and reactive oxygen species (ROS), which are triggered by various stimuli, are two classes of key signaling molecules activating downstream signaling pathways to cope with stresses. Emerging evidence suggests that the interplay of RNS and ROS was regulated by protein S-nitrosylation in improving stress responses in plants (Yang et al., 2015). Protein S-nitrosylation positively regulates the activity of ascorbate peroxidase (Yang et al., 2015), but negatively regulates the activity of peroxiredoxin II E (Romero-Puertas et al., 2007) and NADPH oxidase (RBOH) (Yun et al., 2011), thereby modulating the ROS signaling and oxidative stress tolerance in stress conditions. When plants are exposed to unfavorable environmental conditions, the phytohormone in response to stressors has eventually unraveled their potentials in coffering tolerance to such conditions including sodic alkaline stress (Ryu et al., 2015). For example, the S-nitrosylation of TRANSPORT INHIBITOR RESPONSE 1 (TIR1) in auxin signaling (Terrile et al., 2012) and *Arabidopsis* histidine phosphotransfer protein 1 (AHP1) in cytokinin signaling (Feng et al., 2013) were separately reported to illustrate a mechanism by which RNS signaling and phytohormone signaling coordinate plant growth, development and stress tolerance. As an important stress response phytohormone, abscisic acid (ABA) signaling pathway was also influenced by protein S-nitrosylation (Prakash et al., 2019). S-nitrosylation of the basic leucine zipper-type transcription factor ABI5 at Cys 153 facilitates its degradation through CULLIN4-based and KEEP ON GOING E3 ligases, and inhibits the ABA signaling (Albertos et al., 2015). Furthermore, NO negatively regulates ABA signaling in guard cells by S-nitrosylation of open stomata 1 (OST1) at Cys 137 to regulate the drought stress tolerance (Wang et al., 2015). More interesting, there is a sensible feedback regulation for the activity of GSNOR by S-nitrosylation itself. NO can control its own generation and scavenging by modulating GSNOR activity through S-nitrosylation to adapt to nitrate assimilation (Frungillo et al., 2014). Additionly, when plants are exposed to hypoxic conditions, NO induces the S-nitrosylation of GSNOR at Cys 10, which causes conformational changes, exposing its AUTOPHAGY-RELATED8 (ATG8)-interacting motif (AIM) accessible by autophagy machinery. Upon binding by ATG8, GSNOR is recruited into the autophagosome and degraded in an AIM-dependent manner to generate more NO to adapt to hypoxia stress (Zhan et al., 2018). All these studies illustrate the importance of S-nitrosylation in the regulation of diverse physiological processes in plants.

Because S-nitrosylation is one of the most important posttranslational modification mechanisms, a growing number of studies about S-nitrosylated proteins using the proteomics approaches have been published (Lindermayr et al., 2005; Fares et al., 2014; Hu et al., 2015). A total of 63 and 52 S-nitrosylated proteins were identified in cell suspension cultures and leaves of *Arabidopsis* by applying exogenous NO donors (Lindermayr et al., 2005). In an independent study, 926 endogenously S-nitrosylated proteins were identified from *Arabidopsis* by a site-specific nitrosoproteomics approach, which is the largest dataset of S-nitrosylated proteins among all organisms to date (Hu et al., 2015). It should be noted that many S-nitrosylated proteins have only been repeatedly identified in *Arabidopsis*. Because of the labile nature of S-nitrosylation and differences in protein sequences among different plants, the identification of S-nitrosylation should be expanded and studied in important crop species. In this study, we used RNA-interference (RNAi) to create several lines of *GSNOR* knockdown tomato plants, which showed excessive accumulation of endogenous NO and sodic alkaline stress-sensitive phenotypes (Fig. 1; this figure was cited from Fig. 3A of Gong et al., 2015.). Through this approach, we hope to identify *GSNOR*-mediated S-nitrosylation that can depict a more comprehensive map of the S-nitrosoproteome in tomato plants and provide important clues on the molecular basis of the sodic alkaline stress sensing mediated by *GSNOR*.

2. Material and methods

2.1. Plant materials and treatments

Tomato self-pollinated homozygous cultivar (*Solanum lycopersicum* L.) was used in this study. *GSNOR* knockdown tomato lines have been established by RNA interference (RNAi) approach, which are available *GSNOR* knockdown plant materials identified by southern blot analysis, quantitative RT-PCR analysis, enzyme activity analysis, as well as Western blot analysis in our previous study (Gong et al., 2015). Five fifteen-day-old seedlings of wild type plants (marked as “WT”) or *GSNOR* knockdown plants (marked as “G”) were transplanted into 5 L black plastic containers containing aerated full Hoagland's nutrient solution. Stress treatments were started after 15 d of pre-culture. The experimental design consisted of a control treatment without $NaHCO_3$ application (marked as “C”) and sodic alkaline stress treatment with 75 mM $NaHCO_3$ (marked as “S”). Thus, there are four treatments together, which are WT plants in control treatment (marked as “WT-C”), *GSNOR* knockdown plants in control treatment (marked as “G-C”), WT plants in sodic alkaline stress (marked as “WT-S”), *GSNOR* knockdown plants in sodic alkaline stress (marked as “G-S”). Five days after treatment, the third true leaves of 50 seedlings in each treatment were taken and mixed abundantly for site-specific nitrosoproteomic analysis. All samples were immediately frozen in liquid nitrogen until protein

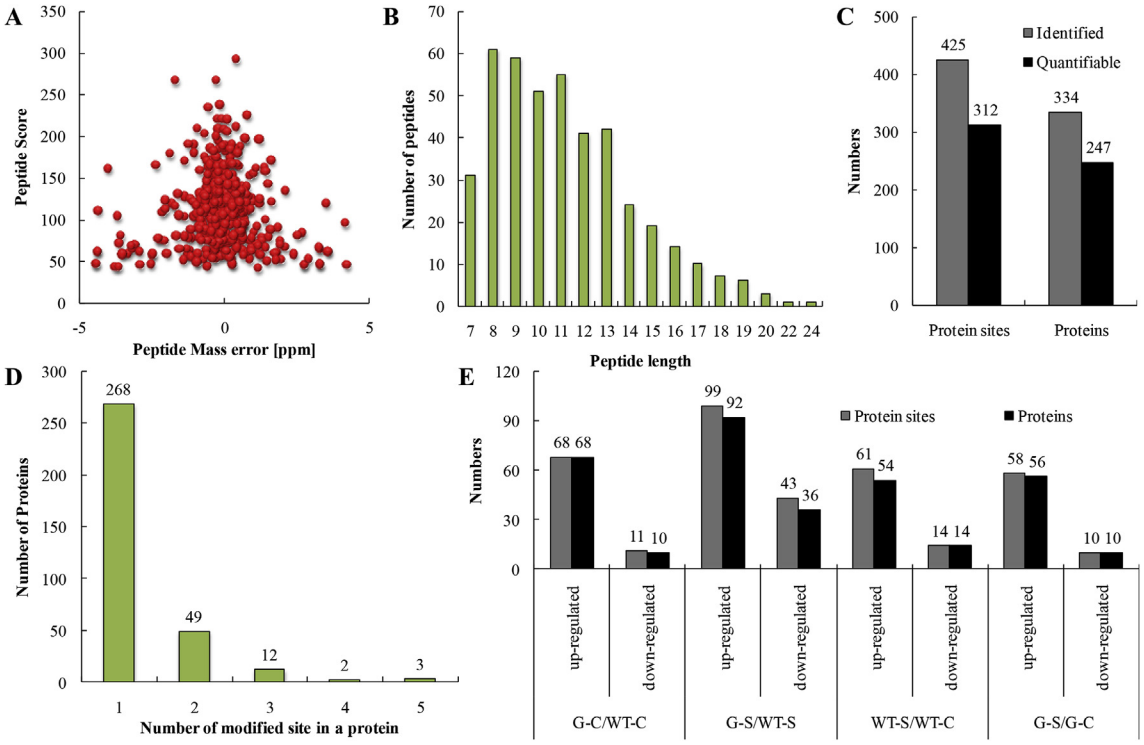

Fig. 2. Basic information of *GSNOR*-mediated S-nitrosylation. (A) QC validation of MS data: mass error distribution of all identified peptides. (B) Distribution of peptide length. (C) Numbers of identified and quantifiable proteins and their sites. (D) Distribution of modified site per protein. (E) Numbers of significantly changed proteins and their sites in different groups.

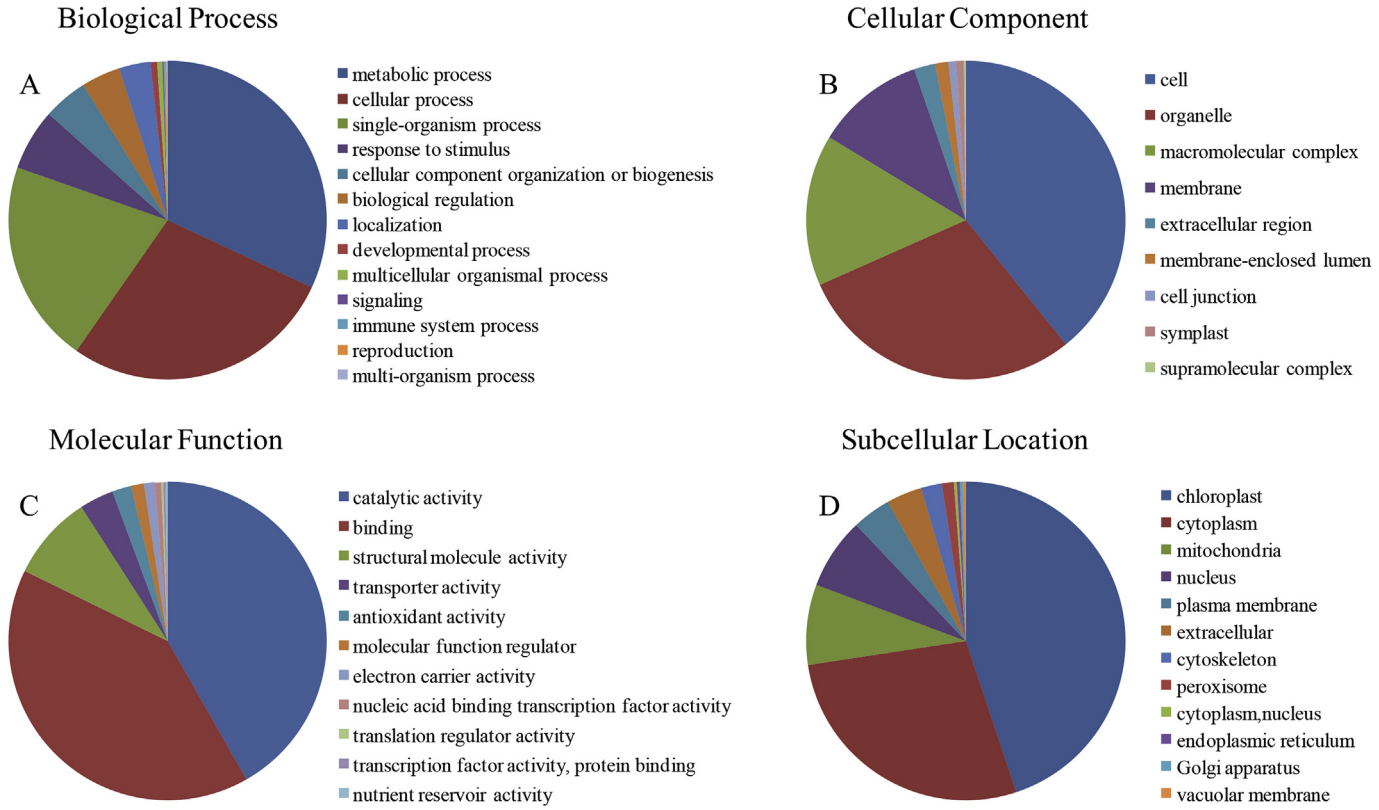

Fig. 3. Functional classification of *GSNOR*-mediated S-nitrosylation. Gene ontology (GO) analyses of S-nitrosylated proteins by (A) biological process, (B) cellular component, (C) molecular function and (D) subcellular location.

extraction.

2.2. Site-specific nitrosoproteomic analysis

Site-specific nitrosoproteomic analysis was performed according to previous studies with some modification (Murry et al., 2012; Su et al., 2013; Guo et al., 2014; Wojdyla et al., 2015). The experimental process was shown as follows:

Protein extraction: The sample was grinded by liquid nitrogen into cell powder and then transferred to a 5 ml centrifuge tube. After that, four volumes of lysis buffer [8 M urea, 1% TritonX-100, 100 mM TEAB (Triethylammonium bicarbonate buffer, Sigma-Aldrich, 17902-100 mL, Saint Louis, USA), 50 mM IAM (Iodoacetamide, Sigma-Aldrich, V900335-5G, Saint Louis, USA), and 1% Protease Inhibitor Cocktail] was added to the cell powder, followed by sonication three times on ice using a high intensity ultrasonic processor. Then the lysate was incubated for 30 min at room temperature in the dark to block free cysteine thiols. The remaining debris was removed by centrifugation at 20,000 × *g* at 4 °C for 10 min. Finally, the protein was precipitated with cold 20% TCA for 2 h at −20 °C. After centrifugation at 12,000 × *g* 4 °C for 10 min, the supernatant was discarded. The remaining precipitate was washed with cold acetone for three times. The protein was redissolved in HES buffer (50 mM TEAB, 1 mM EDTA, 0.1% SDS) and the protein concentration was determined with BCA kit according to the manufacturer's instructions.

Iodo-TMT labelling: Protein labelling was performed according to the manufacturer's protocol for iodo-TMT kit (ThermoFisher Scientific, 90068, Waltham, USA). Briefly, 1 mg protein per condition was resuspended in 1 mL HES buffer. Meanwhile, iodo-TMT reagent was thawed and dissolved in 10 μL MS grade methanol and was added to the protein solution, followed by adding 20 μL of 1 M sodium acscorbate and mixed briefly. The mixture was incubated for 2 h at 37 °C in the dark. The reaction was quenched by adding 40 μL of 0.5 M DTT (20 mM final concentration) and incubating at 37 °C for 15 min without light.

Trypsin digestion: For digestion, the labelled protein was mixed and precipitated with six volumes of pre-chilled (−20 °C) acetone at −20 °C for at least 2 h. After centrifugation at 12,000 × *g* 4 °C for 10 min, the supernatant was discarded. The remaining protein precipitate was washed with cold acetone for three times and dissolved in 8 M urea. The protein solution was reduced with 5 mM dithiothreitol for 30 min at 56 °C and alkylated with 11 mM iodoacetamide for 15 min at room temperature in darkness. The protein sample was then diluted by adding 100 mM TEAB to urea concentration less than 2 M. Finally, trypsin was added at 1 : 50 trypsin-to-protein mass ratio for the first digestion overnight and 1 : 100 trypsin-to protein mass ratio for a second 4 h-digestion. After trypsin digestion, peptide was desalted by Strata X C18 SPE column (Phenomenex) and vacuum-dried.

HPLC fractionation: The sample was then fractionated into fractions by high pH reverse-phase HPLC using Agilent 300 Extend C18 column (5 μm particles, 4.6 mm ID, 250 mm length). Briefly, peptides were first separated with a gradient of 2%–60% acetonitrile in 10 mM ammonium bicarbonate pH 10 over 80 min into 80 fractions, Then, the peptides were combined into 4 fractions and dried by vacuum centrifuging.

LC-MS/MS analysis: The tryptic peptides were dissolved in 0.1% formic acid (solvent A), directly loaded onto a home-made reversed-phase analytical column (15 cm length, 75 μm i.d.). The gradient was comprised of an increase from 6% to 23% solvent B (0.1% formic acid in 98% acetonitrile) over 26 min, 23%–35% in 8 min and climbing to 80% in 3 min then holding at 80% for the last 3 min, all at a constant flow rate of 400 nl min^{-1} on an EASY-nLC 1000 UPLC system. Then, the peptides were subjected to NSI source followed by tandem mass spectrometry (MS/MS) in Q ExactiveTM Plus (Thermo) coupled online to the UPLC. The electrospray voltage applied was 2.0 kV. The m/z scan range was 350–1800 for full scan, and intact peptides were detected in the Orbitrap at a resolution of 70,000. Peptides were then selected for MS/MS using NCE setting as 28 and the fragments were detected in the Orbitrap at a resolution of 17,500. A data-dependent procedure that alternated between one MS scan followed by 20 MS/MS scans with 15.0s dynamic exclusion. Automatic gain control (AGC) was set at 5E4.Fixed first mass was set as 100 m/z.

Database search: The resulting MS/MS data was processed using MaxQuant with integrated Andromeda search engine (v.1.5.2.8). Tandem mass spectra were searched against UniProt *Solanum lycopersicum* L. database concatenated with reverse decoy database. Trypsin/P was specified as cleavage enzyme allowing up to 2 missing cleavages, 5 modifications per peptide and 7 charges. Mass error was set to 10 ppm for precursor ions and 0.02 Da for fragment ions. Carbamidomethylation and iodo-TMT6plex on Cys, oxidation on Met, and acetylation on protein N-terminal were specified as variable modifications. False discovery rate (FDR) thresholds for protein, peptide and modification site were specified at 1%. Minimum peptide length was set at 7. For quantification method, iodo-TMT-6plex was selected. All the other parameters in MaxQuant were set to default values. The site localization probability was set as > 0.75.

Gene ontology (GO) annotation: GO annotation proteome was derived from the UniProt-GOA database (http://www.ebi.ac.uk/GOA/). Firstly, Converting identified protein ID to UniProt ID and then mapping to GO IDs by protein ID. If some identified proteins were not annotated by UniProt-GOA database, the InterProScan soft would be used to annotated protein's GO functional based on protein sequence alignment method. Then proteins were classified by Gene Ontology annotationbased on three categories: biological process, cellular component and molecular function.

KEGG pathway annotation: Firstly, using KEGG online service tools KAAS to annotated protein's KEGG database description (https://www.genome.jp/kaas-bin/kaas_main). Then mapping the annotation result on the KEGG pathway database using KEGG online service tools KEGG mapper (https://www.kegg.jp/kegg/mapper.html).

Subcellular localization: We used wolfpsort a subcellular localization predication soft to predict subcellular localization (http://www.genscript.com/psort/wolf_psort.html). Wolfpsort an updated version of PSORT/PSORT II for the prediction of eukaryotic sequences.

Enrichment of GO analysis: Proteins were classified by GO annotation into three categories: biological process, cellular compartment and molecular function. For each category, a two-tailed Fisher's exact test was employed to test the enrichment of the differentially expressed protein against all identified proteins. The GO with a corrected p-value < 0.05 is considered significant.

Enrichment of pathway analysis: Encyclopedia of Genes and Genomes (KEGG) database was used to identify enriched pathways by a two-tailed Fisher's exact test to test the enrichment of the differentially expressed protein against all identified proteins. The pathway with a corrected p-value < 0.05 was considered significant. These pathways were classified into hierarchical categories according to the KEGG website.

Enrichment-based clustering: We first collated all the categories obtained after enrichment along with their P values, and then filtered for those categories which were at least enriched in one of the clusters with P value < 0.05. This filtered P value matrix was transformed by the function x = −log10 (P value). Finally these x values were z-transformed for each functional category. These z scores were then clustered by one-way hierarchical clustering (Euclidean distance, average linkage clustering) in Genesis. Cluster membership were visualized by a heat map using the “heatmap.2” function from the “gplots” R-package.

Protein-protein interaction network analysis: All interesting protein name identifiers were searched against the STRING database version 10.5 for protein-protein interactions. Only interactions between the proteins belonging to the searched data set were selected, thereby excluding external candidates. STRING defines a metric called “confidence score” to define interaction confidence; we fetched all

interactions that had a confidence score ≥0.7 (high confidence). Interaction network form STRING was visualized in Cytoscape. A graph theoretical clustering algorithm, molecular complex detection (MCODE) was utilized to analyse densely connected regions. MCODE is part of the plug-in tool kit of the network analysis and visualization software Cytoscape.

2.3. Enzyme activity assay

The activity of glyceraldehyde-3-phosphate dehydrogenase (GAPDH) was determined according to Lindermayr et al. (2005). And the activity of ascorbate peroxidase (APX) was determined according to Gong et al. (2015).

3. Results and discussion

3.1. GSNOR is the key scavenger for sodic alkaline stress-induced S-nitrosylation

The expression of *GSNOR* has been identified in all organs in tomato plants (Kubienová et al., 2013). Our previous study indicated that knockdown of *GSNOR* showed sodic alkaline stress-sensitive phenotype; however, overexpression of *GSNOR* could acquire the sodic alkaline stress tolerance (Gong et al., 2015). We also observed that knockdown of *GSNOR* had significantly higher levels of NO and S-nitrosothiols (SNOs) compared with WT plants (Gong et al., 2015). Because the major biological activity of RNS, including NO and SNOs, is protein S-nitrosylation, we reasoned that the increased RNS level should result in more S-nitrosylation of the proteome, which could influence the sodic alkaline stress tolerance in tomato plants. To test this hypothesis, a site-specific nitrosoproteomic assay using iodo-TMT switch labelling was performed to analyse the levels of S-nitrosylated proteins as well as S-nitrosylated protein sites in treatments of WT-C, G-C, WT-S and G-S. First, we checked the mass error of all the identified peptides. The distribution of mass error was near zero and most of them were less than 0.02 Da, which means the mass accuracy of the MS data fit the requirements (Fig. 2A). Second, the length of most peptides distributed from 8 to 13 amino acids, which is consistent with the typical size tryptic peptides (Fig. 2B), indicating that sample preparation was acceptable. A total of 334 proteins with 425 protein sites were identified in this approach, covering 247 quantifiable proteins and 312 quantifiable protein sites (Fig. 2C; Supplementary Table S1). Among these proteins, 268 proteins with 1 sites, 49 proteins with 2 sites, 12 proteins with 3 sites, 2 proteins with 4 sites, and 3 proteins with 5 sites were separately identified (Fig. 2D). Based on a 95% confidence level, cutoff values of 1.20-fold for up-regulation and 0.83-fold for down-regulation were used to define a protein or protein site as being influenced by *GSNOR* or sodic alkaline stress. Using these criteria, a total of 78 proteins with 79 protein sites were identified in G-C/WT-C, including 68 proteins with 68 sites that were up-regulated and 10 proteins with 11 sites that were down-regulated (Fig. 2E). Similarly, 128 proteins with 142 protein sites were identified in G-S/WT-S, including 92 proteins with 99 sites that were up-regulated and 36 proteins with 43 sites that were down-regulated (Fig. 2E). 68 proteins with 75 protein sites were identified in WT-S/WT-C, including 54 proteins with 61 sites that were up-regulated and 14 proteins with 14 sites that were down-regulated (Fig. 2E). 66 proteins with 68 protein sites were identified in G-S/G-C, including 56 proteins with 58 sites that were up-regulated and 10 proteins with 10 sites that were down-regulated (Fig. 2E). Together, more detailed data of these significantly changed proteins and sites is shown in Supplementary Table S2.

In these four comparable groups, we used groups of G-C/WT-C and G-S/WT-S to analysis the effects of knockdown *GSNOR* on protein S-nitrosylation in both control and sodic alkaline stress conditions. And groups of WT-S/WT-C and G-S/G-C were used to analysis the effects of sodic alkaline stress on protein S-nitrosylation in both WT plants and *GSNOR* knockdown plants. Important, 160 proteins with 167 protein sites were significantly up-regulated, and only 46 proteins with 54 protein sites were significantly down-regulated by the effects of knockdown *GSNOR* on protein S-nitrosylation (Fig. 2E). Similarly, 110 proteins with 119 protein sites were significantly up-regulated, and only 24 proteins with 24 protein sites were significantly down-regulated by the effects of sodic alkaline stress on protein S-nitrosylation (Fig. 2E). These results reveal that the process of protein S-nitrosylation can be activated by knockdown of *GSNOR* or sodic alkaline stress, which was consistent with our previous results of NO and SNOs assay (Gong et al., 2015). Additionally, knockoff (Hu et al., 2015) and knockdown (Frungillo et al., 2013) of *GSNOR* have also been confirmed to improve levels of NO and protein S-nitrosylation in *Arabidopsis*. Not only sodic alkaline stress, but also salt (Tanou et al., 2012; Camejo et al., 2013; Jain et al., 2018), low temperature (Abat and Deswal, 2009; Sehrawat and Deswal, 2014), high-light (Lin et al., 2012), and oxidative stress (Lin et al., 2012) have been demonstrated to cause protein S-nitrosylation in several plants. These results indicate that stress conditions usually induce major modulations of RNS levels to improve protein S-nitrosylation. So, we conjectured that *GSNOR* plays critical roles in scavenging sodic alkaline stress-induced GSNO, NO and SNOs to decrease the levels of protein S-nitrosylation in tomato plants.

3.2. Functional classification of S-nitrosylated proteins

GO analysis was performed to illustrate the regulatory mechanism of S-nitrosylated proteins in specific biological processes of WT and GSNOR knockdown plants under both control and sodic alkaline stress conditions (Fig. 3). Totally, 754 S-nitrosylated proteins were subjected to biological process (Fig. 3A), covering a wide range of metabolic process (31.96%), cellular process (27.72%), single-organism process (20.69%), response to stimulus (6.23%), cellular component organization or biogenesis (4.51%), biological regulation (3.98%), localization (3.18%), and other six processes (1.72%). For cellular component, 515 S-nitrosylated proteins were classified (Fig. 3B), such as cell (39.22%), organelle (29.13%), macromolecular complex (15.34%), membrane (11.07%), extracellular region (2.14%), and other four processes (3.11%). And 426 S-nitrosylated proteins were subjected to molecular function (Fig. 3C), including catalytic activity (41.77%), binding (40.78%), structural molecule activity (8.66%), transporter activity (3.46%), antioxidant activity (1.95%), molecular function regulator (1.41%), electron carrier activity (1.17%), and other four processes (1.41%).

The most enriched categories of these S-nitrosylated proteins were related to various metabolic, cellular and catalytic processes (Fig. 3A–C). It is possibly due to the relatively high abundance of these proteins and also implies that the basal metabolism, cellular component, and catalytic activity are regulated by S-nitrosylation. With similar treatment, we previously observed that sodic alkaline stress indeed decreased the basal metabolism of photosynthesis, respiration in both physiological (Gong et al., 2013 and 2014b) and proteomic (Gong et al., 2014a) levels, destroyed the cellular component including chloroplast, mitochondrion, membranal component, and so on (Gong et al., 2014c; Saxena et al., 2018). Moreover, 47 S-nitrosylated proteins with 53 S-nitrosylated sites have been identified in the response to stimulus (Supplementary Table S3). Among these proteins, only one protein, calcium sensing receptor (CAS; K4BKU7), involving stress response signaling has been identified (Supplementary Table S3), which implies that the crosstalk between RNS and Ca^{2+} signaling in plants stress tolerance maybe depend on this post-translational modifications. As a common toxic metabolite, ROS bust can be detected nearly under all stress conditions (Turkan, 2018). And 9 ROS-scavenging enzymes, including 2 superoxide dismutase (SOD; Q9SBJ4 and Q7XAV2), 2 catalase (CAT; P30264 and Q9XHH3); 2 ascorbate peroxidase (APX; Q3I5C4 and Q09Y77), 1 dehydroascorbate reductases (DHAR; Q4VDN8), and 2 thioredoxin (TRX; K4BVS6 and K4DCR6), were

identified as S-nitrosylated proteins (Supplementary Table S3), supporting the notion of active interactions between RNS- and ROS-mediated signaling pathways in stress tolerance. In addition, three key enzymes of NO metabolism, GSNOR (D2Y3F4), nitrite reductase (NIR; K4B378) and bifunctional nitrilase/nitrile hydratase (NIT; K4DA30), have also been identified in this S-nitrosoproteome, which have been consistent with the results of biotin-switch assay in previous study (Frungillo et al., 2014), suggesting the involvement of feedback regulation in NO-mediated S-nitrosylation. Importantly, previous study indicated that S-nitrosation of conserved cysteines modulates activity and stability of GSNOR (Guerra et al., 2016. Tichá et al., 2017). Collectively, these data suggest a mechanism for NO signal transduction in which GSNOR nitrosation and inhibition transiently permit GSNO accumulation.

GO subcellular location analysis (Fig. 3D) revealed that the S-nitrosylated proteins were significantly enriched in the chloroplast (44.28%), followed by the cytoplasm (27.71%), mitochondria (8.13%), nucleus (7.23%), plasma membrane (3.92%), extracellular (3.61%), cytoskeleton (2.11%), peroxisome (1.20%), and other four subcellular components (1.20%). GO subcellular location analysis of protein S-nitrosylation in *Arabidopsis* also revealed a similar distribution pattern of the first five subcellular components (Hu et al., 2015). One hand, because chloroplast occupies the most part of mesophyll cell, high abundance of proteins localized in the chloroplast have been identified in not only this proteome but also nearly all proteome of leaves (Hu et al., 2015; Zhou et al., 2018). The other hand, the most abundant S-nitrosylated proteins were obtained in chloroplast, suggesting that the physiological activities associated with the photosynthetic organelle are extensively regulated by *GSNOR*-modulated protein S-nitrosylation. Moreover, chloroplast is one of the most drastic oxidoreduction-based subcellular organelles, where the series of redox-based protein S-nitrosylation for photosynthetic regulation take place in (Zaffagnini et al., 2012). Because the chloroplast is a major site for metabolic process of plants, this result is consistent with the GO analysis (Fig. 3A).

3.3. Venn diagram showing the relationship of overlapping S-nitrosylated proteins in different treatments

The venn diagram analysis (Fig. 4 and Supplementary Table S1) was performed with the aim to make sure that what was happened under the levels of protein S-nitrosylation when tomato plants were exposed to sodic alkaline stress conditions, as well as how *GSNOR* influenced the sodic alkaline stress tolerance. Totally, 59 proteins (35.0%) were significantly regulated by *GSNOR* under control and stress conditions (G-C/WT-C and G-S/WT-S), which can be understood as the important S-nitrosylated proteins influenced by *GSNOR* effect. 26 proteins (15.4%) were significantly regulated by sodic alkaline stress in both WT and *GSNOR* knockdown plants (WT-S/WT-C and G-S/G-C), which can be understood as the important S-nitrosylated proteins influenced by stress effect. More importantly, 11 proteins (6.5%) were significantly regulated in all four comparative groups, which can be used to explain that how knockdown of *GSNOR* results a sodic alkaline stress-sensitive phenotype through protein S-nitrosylation.

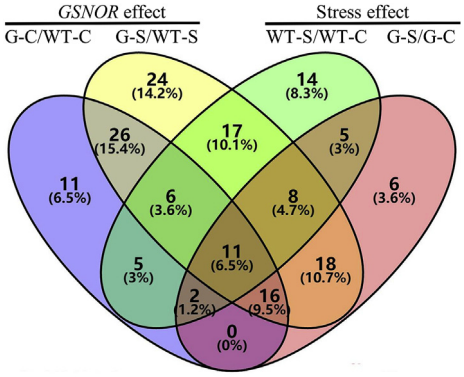

Fig. 4. Venn diagram showing the number of overlapping S-nitrosylated proteins that were significantly different between wild type (WT) and *GSNOR* knock down (G) tomato plants without (C) and with sodic alkaline stress (S) conditions.

The above-mentioned 11 S-nitrosylated proteins (Table 1) were distributed in 4 sodic alkaline stress tolerance-related processes, including photosynthesis, proline metabolism, ethylene signaling and protein stability. Large numbers of studies have demonstrated that soidc alkaline stress can induce chlorosis and the developmental disabilities of chloroplast resulting decreased photosynthesis in not only tomato (Gong et al., 2013, 2014c and 2015) but also in other plants (Li et al., 2018; Mir et al., 2018). Plastid-lipid associated protein (PAP; A0RZD0), Ribulose bisphosphate carboxylase (Rubisco; P07180) and NADH dehydrogenase (Ndh; K4BBN1) were identified to maintain the structural stability of plastid lipid bodies in chloroplast (Smith et al., 2000) and control the energy conversion among luminous energy, actively chemical energy and stably chemical energy, suggesting that key components of photosynthesis are extensively regulated by S-nitrosylation. As a communally protective mechanism, the regulatory changes of proline and its rate-limiting enzyme (pyrroline-5-carboxylate reductase; PYCR) can be observed in nearly all osmotic stress including sodic alkaline stress (Lv et al., 2014). We observed that the S-nitrosylated patterns of PYCR (K4B7J6) were 1.24-fold in G-C/WT-C, 2.07-fold in G-S/WT-S, 0.79-fold in WT-S/WT-C, and 1.32-fold in G-S/G-C. These changes showed that the S-nitrosylated level of PYCR was down-regulated by sodic alkaline stress in WT plants, however, knockdown of *GSNOR* significantly induced the S-nitrosylation of PYCR in both control and stress condition. Thus, we conjecture that the down-regulation of PYCR S-nitrosylation is an adaptive mechanism for tomato plants against sodic alkaline stress. So, the significantly up-regulation of PYCR S-nitrosylation by knockdown of *GSNOR* can be responsible for the sodic alkaline stress-sensitive phenotype. However, as a key pathway, this subtle regulatory mechanism of proline metabolism by S-nitrosylation should be verified in future study. Ethylene is often associated with sodic alkaline stress responses (Li et al., 2015). The last step of ethylene biosynthesis was regulated by *GSNOR* through S-nitrosylation 1-aminocyclopropane-1-carboxylate oxidase (ACO; K4BNV4). In addition, two kinds of molecular chaperones (K4C227 and K4D9L5) have been identified to bind with other proteins against stress-induced protein destroy (Martin et al., 1992). Taken together, knockdown of *GSNOR* encourage sodic alkaline stress-induced S-nitrosylation of these key stress response proteins, causing the resistant reduction.

3.4. KEGG pathway enrichment analysis of S-nitrosylated proteins

The KEGG online service tools highlighted which protein categories were up- or down-regulated in each pairwise comparison (Fig. 5; Supplementary Table S5). For stress effect, four significantly enriched pathways, including amino sugar and nucleotide sugar metabolism, MAPK signaling pathway, sulfur metabolism, and pyruvate metabolism, were identified in WT-S/WT-C or G-S/G-C. Except these four pathways, another three pathways of valine, leucine and isoleucine degradation, glycolysis/gluconeogenesis, and fatty acid degradation were also identified in G-C/WT-C or G-S/WT-S for *GSNOR* effect.

Stressor-specific activation of MAPK-related pathway has been detected when plants are subjected to biotic or abiotic stress (Ding et al., 2018). Several studies of *Arabidopsis* showed that MAPK pathway deletion of *mekk1*, *mkk2*, *mpk3*, *mpk4* or *mpk6* had reduced tolerance to salt stress, and overexpression of these genes exhibited enhanced tolerance to salt stress (Teige et al., 2004; Pitzschke et al., 2014; Wang et al., 2014). There are also some evidence about the relationship between NO and MAPK signaling. Several physiological reaction and stress response that regulated by MAPK can be activated by NO in both animal and plants (Kubo et al., 1998; Pagnussat et al., 2004; Zhang

Table 1
Selected candidates of identified S-nitrosylated proteins from all four comparative groups.

Protein accession	Position of Cys	Protein names	G-C/WT-C	G-S/WT-S	WT-S/WT-C	G-S/G-C
A0RZD0	174	Inducible plastid-lipid associated protein	3.80	3.16	1.80	1.50
K4BBN1	148	NADH dehydrogenase	1.44	1.44	1.24	1.24
P07180	169	Ribulose bisphosphate carboxylase small chain	0.77	0.83	1.24	1.34
K4B7J6	5	pyrroline-5-carboxylate reductase	1.24	2.07	0.79	1.32
K4BNV4	172	1-aminocyclopropane-1-carboxylate oxidase	2.00	1.78	2.02	1.80
K4C227	135	chaperonin	1.55	1.54	1.22	1.22
K4D9L5	319	heat shock cognate 70 kDa protein	1.57	2.08	1.25	1.66
Q7Y0S1	231	Chitinase	3.05	7.99	1.42	3.71
Q9M4X2	304	Putative cytochrome P450	1.31	1.23	0.75	0.70
K4BSP6	106	uncharacterized protein	1.65	1.60	1.33	1.29

et al., 2007). However, until now, there is no evidence about the involvement of S-nitrosylation in MAPK signaling pathway. In the present study, we discovered four MAPK-related proteins (K4D1H0, Q05538, Q0H8U4 and Q7Y0S1) that can be regulated by S-nitrosylation, which may be helpful for us to reveal the regulatory mechanism of NO to MAPK signaling pathway.

Additionally, many metabolic enzymes were identified as potential candidates for S-nitrosylation in GSNOR effect treatments. Nine proteins of the glycolysis/gluconeogenesis (K4CHR6, K4CB11, K4CEP2, Q42887, Q8GT30, D2Y3F4, Q9FR11, K4BKR7, K4D5K6), as well as eight proteins of pyruvate metabolism (K4AXU0, Q8GT30, K4CEU2, K4DBR8, Q9FR11, K4CG46, K4DCV3, K4BKR7) are sensitive to S-nitrosylation, among which, only glyceraldehyde-3-phosphate dehydrogenase (GAPDH; K4CB11) with a Cys residue in the active center has been reported to be inhibited by GSNO (Mohr et al., 1996; Lindermayr et al., 2005). Unfortunately, little evidence can be found to reveal the relationship between S-nitrosylation and other enzymes' activities. Our previous studies indicated that glycolysis and tricarboxylic acid cycle pathway is important for energy support when the tomato plants are exposed to sodic alkaline stress (Gong et al., 2014a and 2014b). Thus, knockdown of *GSNOR* leading to low activity of GAPDH by S-nitrosylation can be partly responsible for the sensitive stress phenotype through regulating glycolysis-controlled energy metabolism. To our interesting, three proteins of fatty acid degradation pathway (K4BKR7, D2Y3F4, K4CEU2) can be observed in *GSNOR* effect treatments, which supports the gluconeogenesis pathway. This result implied that basic energy metabolism is regulated by *GSNOR* through S-nitrosylation, which is the common problem for stress response and life force.

3.5. Validation of the nitrosoproteomic by analyzing two identified enzymes

Several candidates of our nitrosoproteomic for S-nitrosylation have been reported in previous studies, including their enzyme activity or protein structure. We have chosen GAPDH and APX (Fig. 6A) as the model enzymes since an easy and fast activity assay as well as confirmed S-nitrosylation for these two enzymes are already established (Lindermayr et al., 2005; Yang et al., 2015). Crude extracts of leaves were incubated with different concentrations of GSNO. The activities of GAPDH (Fig. 6B) and APX (Fig. 6D) were reduced and increased separately by applying different concentrations of GSNO. Addition of DTT to these two enzymes completely restored the activities (Fig. 6B,D), confirming that the effect of the GSNO was due to S-nitrosylation of one or more critical Cys residues. More importantly, genetic manipulation of *GSNOR* showed similar results as exogenous application of GSNO (Fig. 6B–E). In particular, our observation of activities about GAPDH and APX, which were regulated by S-nitrosylation, showed consistent results when compared with previous studies (Lindermayr et al., 2005; Yang et al., 2015). Taken together, these results suggest that our nitrosoproteomic for S-nitrosylation is available for future study.

4. Conclusion

This study provides a global and comparative analysis of S-nitrosoproteome regulation by *GSNOR* and offers further insights into the dynamics of individual S-nitrosylated protein sites in tomato plants under both control and sodic alkaline stress conditions. Most of the S-nitrosylated proteins in *GSNOR* knockdown plants were significantly up-regulated, which demonstrated the important roles of *GSNOR* in the degradation of S-nitrosylation during NO-mediated stress response in tomato. Based on the data of S-nitrosoproteome in the current as well as our previous studies (Gong et al., 2015), knockdown of *GSNOR* exacerbated the negative effects of sodic alkaline stress on tomato plants by S-nitrosylation. Numbers of studies indicated that NO can also be a double-edged sword, either acting as a defense signal to improve stress tolerance or inducing serious nitrosative damage to increase stress sensibility (Gong et al., 2015; Chamizo-Ampudia et al., 2017; Sami et al., 2018; Seth et al., 2018). As shown in Fig. 7A, we found that there is a sensitive feedback control system in *GSNOR*-modulated S-nitrosylation, which control NO homeostasis to decide the degree of stress response. Additionally, some proteins involving Ca^{2+}, ethylene and MAPK signaling pathway have also been identified in this data, which can be responsible for *GSNOR*-modulated systemic resistance for stressors. As specific response for sodic alkaline stress, *GSNOR*-modulated S-nitrosylation was also involved in the processes of stress-induced ROS generation, dehydration and enfeeblement. However, we did not found the S-nitrosylated proteins about Na^{+} detoxification process, which is consistent with the bioinformatics analysis of Salt-Overly-Sensitive (SOS) family proteins (Supplementary Fig. 1). To our knowledge for the first time, our results identified many novel S-nitrosylated protein sites in tomato plants. For example, Cys-172 of ACO

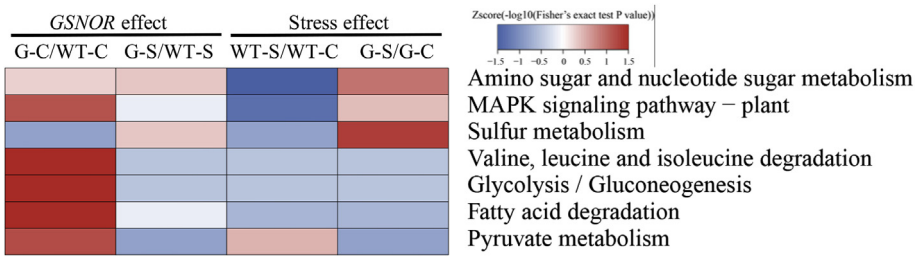

Fig. 5. Heat maps obtained from KEGG pathway enrichment-based cluster analysis.

A

Protein accession	Position of Cys	Protein names	G-C/WT-C	G-S/WT-S	WT-S/WT-C	G-S/G-C
K4CB11	50	Glyceraldehyde-3-phosphate dehydrogenase (GAPDH)	1.40	1.26	n.d.	n.d.
	363		n.d.	0.67	1.48	n.d.
Q3I5C4	4	Ascorbate peroxidase (APX)	n.d.	1.52	n.d.	1.41
	32		1.49	1.56	n.d.	n.d.

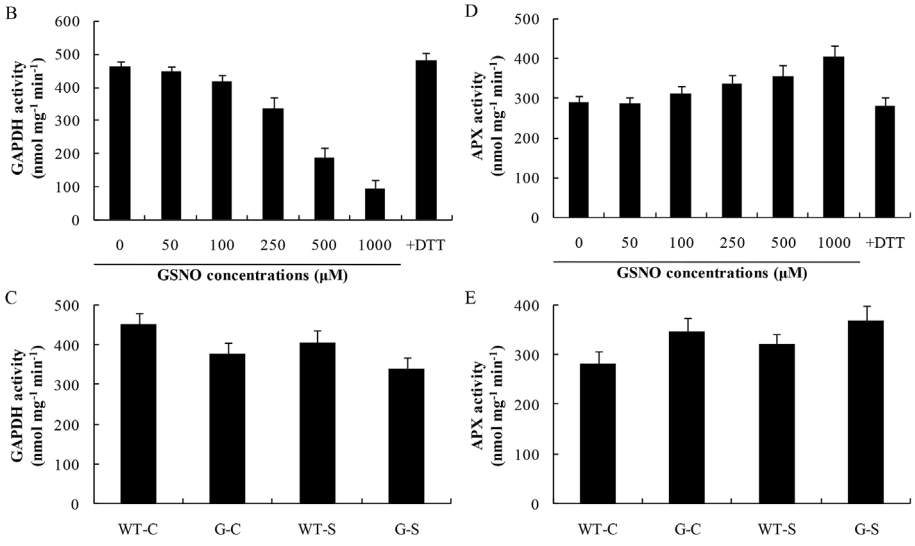

Fig. 6. (A) Information of selected candidates. (B and D) Effect of GSNO and DTT on GAPDH and APX activities. Crude extracts of Arabidopsis cell cultures were treated with different concentrations. (C and E) The activities of GAPDH and APX under different treatments. The columns represent the mean values ± SD (n = 3).

and Cys-5 of PYCR was characterized as an S-nitrosylation site (Fig. 7B), and this two proteins play a key role in sodic alkaline stress tolerance by regulating ethylene and proline biosynthesis. The provided data set may serve as an important resource for the functional analysis of S-nitrosylation in tomato and facilitate the elucidation of the sodic alkaline stress tolerance regulated by NO signaling. However, it should be pointed out that some changes unveiled by omics in this study also needs further study.

Author contributions

BG and QS designed the project; BG performed the experiments and writing; QS contributed to manuscript editing.

Acknowledgements

This work was supported by the National Natural Science

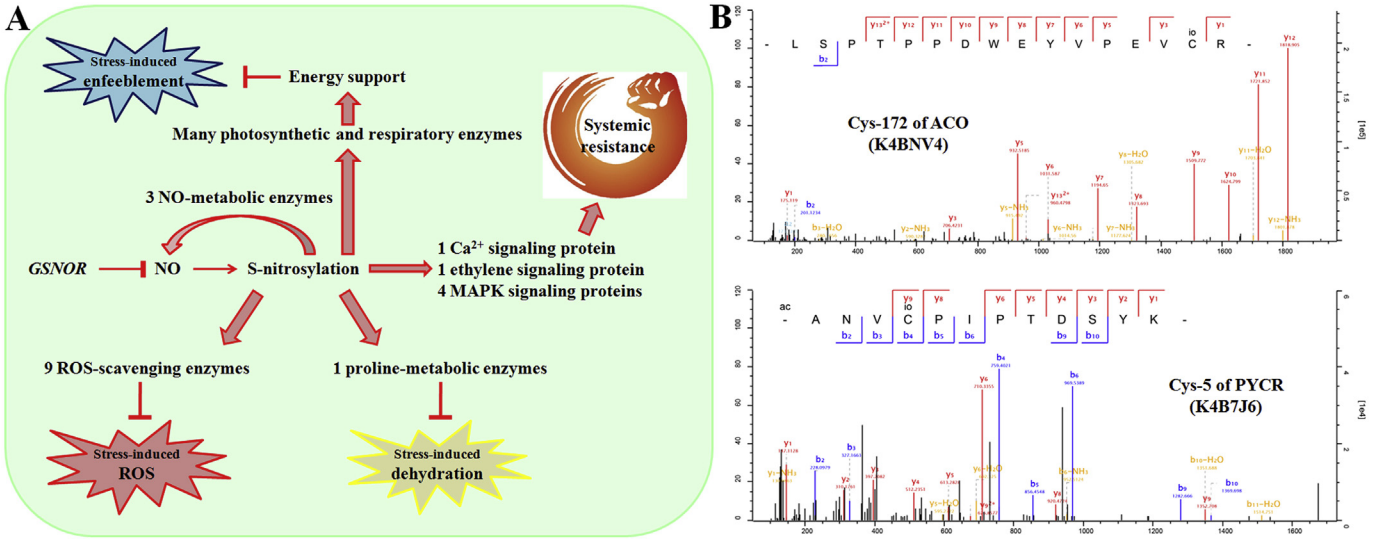

Fig. 7. (A) A model for the influence of sodic alkaline stress tolerance by GSNOR-mediated S-nitrosylation in tomato plants. The information of proteins was shown as follows: 3 NO-metabolic enzymes (D2Y3F4, K4B378 and K4DA30); 1 Ca2+ signaling protein (K4BKU7); 1 ethylene signaling protein (K4BNV4); 4 MAPK signaling proteins (K4D1H0, Q05538, Q0H8U4 and Q7Y0S1); 9 ROS-scavenging enzymes (Q9SBJ4, Q7XAV2, P30264, Q9XHH3, Q3I5C4, Q09Y77, Q4VDN8, K4BVS6 and K4DCR6); 1 proline-metabolic enzymes (K4B7J6); many photosynthetic and respiratory enzymes (too much, the protein ID was not shown). (B) Two examples of mass spectrometric identification of Cys-172 of ACO (K4BNV4) and Cys-5 of PYCR (K4B7J6) as S-nitrosylated residues by site-specific proteomics. The list of fragment ion masses always contains the singly charged b- and y-ions, and occasionally water and ammonia losses.

Foundation of China (31872943 and 31501779), the Shandong Province Modern Agricultural Technology System (SDAIT-05-05).

Appendix A. Supplementary data

Supplementary data to this article can be found online at https://doi.org/10.1016/j.plaphy.2019.06.020.

References

Abat, J.K., Deswal, R., 2009. Differential modulation of S-nitrosoproteome of *Brassica juncea* by low temperature: change in S-nitrosylation of Rubisco is responsible for the inactivation of its carboxylase activity. Proteomics 9, 4368–4380.

Albertos, P., Romero-Puertas, M.C., Tatematsu, K., Mateos, I., Sánchez-Vicente, I., Nambara, E., Lorenzo, O., 2015. S-nitrosylation triggers ABI5 degradation to promote seed germination and seedling growth. Nat. Commun. 6, 8669.

Begara-Morales, J.C., Sánchez-Calvo, B., Luque, F., Leyva-Pérez, M.O., Leterrier, M., Corpas, F.J., Barroso, J.B., 2014. Differential transcriptomic analysis by RNA-Seq of GSNO-responsive genes between Arabidopsis roots and leaves. Plant Cell Physiol. 55, 1080–1095.

Camejo, D., Romero-Puertas, M.C., Rodríguez-Serrano, M., Sandalio, L.M., Lázaro, J.J., Jiménez, A., Sevilla, F., 2013. Salinity-induced changes in S-nitrosylation of pea mitochondrial proteins. J. Proteomics 79, 87–99.

Cellini, A., Corpas, F.J., Barroso, J.B., Masia, A., 2011. Nitric oxide content is associated with tolerance to bicarbonate-induced chlorosis in micropropagated *Prunus* explants. J. Plant Physiol. 168, 1543–1549.

Chamizo-Ampudia, A., Sanz-Luque, E., Llamas, A., Galvan, A., Fernandez, E., 2017. Nitrate reductase regulates plant nitric oxide homeostasis. Trends Plant Sci. 22, 163.

Ding, H., He, J., Wu, Y., Wu, X., Ge, C., Wang, Y., Zhong, S., Peiter, E., Liang, J., Xu, W., 2018. The tomato mitogen-activated protein kinase *SlMPK1* is as a negative regulator of the high temperature stress response. Plant Physiol. 177, 633–651.

Fares, A., Nespoulous, C., Rossignol, M., Peltier, J.B., 2014. Simultaneous identification and quantification of nitrosylation sites by combination of biotin switch and ICAT labeling. Plant Proteomics 609–620.

Feechan, A., Kwon, E., Yun, B.W., Wang, Y., Pallas, J.A., Loake, G.J., 2005. A central role for S-nitrosothiols in plant disease resistance. Proc. Natl. Acad. Sci. U.S.A. 102, 8054–8059.

Feng, J., Wang, C., Chen, Q., Chen, H., Ren, B., Li, X., Zuo, J., 2013. S-nitrosylation of phosphotransfer proteins represses cytokinin signaling. Nat. Commun. 4, 1529.

Frungillo, L., de Oliveira, J.F.P., Saviani, E.E., Oliveira, H.C., Martínez, M.C., Salgado, I., 2013. Modulation of mitochondrial activity by S-nitrosoglutathione reductase in *Arabidopsis thaliana* transgenic cell lines. B.B.A.-Bioenergetics 1827, 239–247.

Frungillo, L., Skelly, M.J., Loake, G.J., Spoel, S.H., Salgado, I., 2014. S-nitrosothiols regulate nitric oxide production and storage in plants through the nitrogen assimilation pathway. Nat. Commun. 5, 5401.

Gong, B., Li, X., VandenLangenberg, K.M., Wen, D., Sun, S., Wei, M., Li, Y., Yang, F., Shi, Q., Wang, X., 2014c. Overexpression of S-adenosyl-$_L$-methionine synthetase increased tomato tolerance to alkali stress through polyamine metabolism. Plant Biotechnol. J. 12, 694–708.

Gong, B., Wen, D., Bloszies, S., Li, X., Wei, M., Yang, F., Shi, Q., Wang, X., 2014b. Comparative effects of NaCl and $NaHCO_3$ stresses on respiratory metabolism, antioxidant system, nutritional status, and organic acid metabolism in tomato roots. Acta Physiol. Plant. 36, 2167–2181.

Gong, B., Wen, D., VandenLangenberg, K., Wei, M., Yang, F., Shi, Q., Wang, X., 2013. Comparative effects of NaCl and $NaHCO_3$ stress on photosynthetic parameters, nutrient metabolism, and the antioxidant system in tomato leaves. Sci. Hortic. 157, 1–12.

Gong, B., Wen, D., Wang, X., Wei, M., Yang, F., Li, Y., Shi, Q., 2015. S-nitrosoglutathione reductase modulated redox signaling controls sodic alkaline stress responses in *Solanum lycopersicum* L. Plant Cell Physiol. 56, 790–802.

Gong, B., Zhang, C., Li, X., Wen, D., Wang, S., Shi, Q., Wang, X., 2014a. Identification of NaCl and $NaHCO_3$ stress responsive proteins in tomato roots using iTRAQ-based analysis. Biochem. Bioph. Res. Co. 446, 417–422.

Guerra, D., Ballard, K., Truebridge, I., Vierling, E., 2016. S-nitrosation of conserved cysteines modulates activity and stability of S-nitrosoglutathione reductase (GSNOR). Biochemistry 55, 2452–2464.

Guo, J., Gaffrey, M.J., Su, D., Liu, T., Camp II, D.G., Smith, R.D., Qian, W.J., 2014. Resin-assisted enrichment of thiols as a general strategy for proteomic profiling of cysteine-based reversible modifications. Nat. Protoc. 9, 64–75.

Gusarov, I., Nudler, E., 2018. Protein S-nitrosylation: enzymatically controlled, but intrinsically unstable, post-translational modification. Mol. Cell 69, 351–353.

Hu, J., Huang, X., Chen, L., Sun, X., Lu, C., Zhang, L., Wang, Y., Zuo, J., 2015. Site-specific nitrosoproteomic identification of endogenously S-nitrosylated proteins in Arabidopsis. Plant Physiol. 167, 1731–1746.

Jain, P., von Toerne, C., Lindermayr, C., Bhatla, S.C., 2018. S-nitrosylation/denitrosylation as a regulatory mechanism of salt stress sensing in sunflower seedlings. Physiol. Plantarum 162, 49–72.

Kubienová, L., Kopečný, D., Tylichová, M., Briozzo, P., Skopalová, J., Šebela, M., Navrátil, M., Tâche, R., Luhová, L., Barroso, J.B., Petřivalský, M., 2013. Structural and functional characterization of a plant S-nitrosoglutathione reductase from *Solanum lycopersicum*. Biochimie 95, 889–902.

Kubo, T., Saito, E., Hanada, M., Kambe, T., Hagiwara, Y., 1998. Evidence that angiotensin II, endothelins and nitric oxide regulate mitogen-activated protein kinase activity in rat aorta. Eur. J. Pharmacol. 347, 337.

Leterrier, M., Chaki, M., Airaki, M., Valderrama, R., Palma, J.M., Barroso, J.B., Corpas, F.J., 2011. Function of S-nitrosoglutathione reductase (GSNOR) in plant development and under biotic/abiotic stress. Plant Signal. Behav. 6, 789–793.

Li, J., Xu, H.H., Liu, W.C., Zhang, X.W., Lu, Y.T., 2015. Ethylene inhibits root elongation during alkaline stress through *AUXIN1* and associated changes in auxin accumulation. Plant Physiol. 168, 1777–1791.

Li, N., Liu, H., Sun, J., Zheng, H., Wang, J., Yang, L., Zhao, H., Zou, D., 2018. Transcriptome analysis of two contrasting rice cultivars during alkaline stress. Sci. Rep. 8, 9586.

Lin, A., Wang, Y., Tang, J., Xue, P., Li, C., Liu, L., Hu, B., Yang, F., Loake, G.J., Chu, C., 2012. Nitric oxide and protein S-nitrosylation are integral to hydrogen peroxide-induced leaf cell death in rice. Plant Physiol. 158, 451–464.

Lindermayr, C., Saalbach, G., Durner, J., 2005. Proteomic identification of S-nitrosylated proteins in Arabidopsis. Plant Physiol. 137, 921–930.

Lv, B.S., Li, X.W., Ma, H.Y., Yang, H.Y., Wei, L.X., Lv, H.Y., Jiang, C.J., Liang, Z.W., 2014. Different modes of proline accumulation in response to saline-alkaline stress factors in rice (*Oryza sativa* L.). Res. Crop 15, 14–21.

Malik, S.I., Hussain, A., Yun, B.W., Spoel, S.H., Loake, G.J., 2011. *GSNOR*-mediated denitrosylation in the plant defence response. Plant Sci. 181, 540–544.

Martin, J., Horwich, A.L., Hartl, F.U., 1992. Prevention of protein denaturation under heat stress by the chaperonin Hsp60. Science 258, 995.

Mir, M.A., John, R., Alyemeni, M.N., Alam, P., Ahmad, P., 2018. Jasmonic acid ameliorates alkaline stress by improving growth performance, ascorbate glutathione cycle and glyoxylase system in maize seedlings. Sci. Rep. 8, 2831.

Mohr, S., Stamler, J.S., Brune, B., 1996. Posttranslational modification of glyceraldehyde-3-phosphate dehydrogenase by S-nitrosylation and subsequent NADH attachment. J. Biol. Chem. 271, 4209–4214.

Murry, C.I., Uhrigshardt, H., O'Meally, R.N., Van Eyk, J.E., 2012. Identification and quantification of S-nitrosylation by cysteine reactive tandem mass tag switch assay. Mol. Cell. Proteom. 11 M111.013441.

Pagnussat, G.C., Lanteri, M.L., Lombardo, M.C., Lamattina, L., 2004. Nitric oxide mediates the indole acetic acid induction activation of a mitogen-activated protein kinase cascade involved in adventitious root development. Plant Physiol. 135, 279–286.

Pitzschke, A., Datta, S., Persak, H., 2014. Salt stress in Arabidopsis: lipid transfer protein AZI1 and its control by mitogen-activated protein kinase MPK3. Mol. Plant 7, 722–738.

Prakash, V., Singh, V.P., Tripathi, D.K., Sharma, S., Corpas, F.J., 2019. Crosstalk between nitric oxide (NO) and abscisic acid (ABA) signalling molecules in higher plants. Environ. Exp. Bot. 161, 41–49.

Rizza, S., Cardaci, S., Montagna, C., Giacomo, G.D., Zio, D.D., Bordi, M., Maiani, E., Campello, S., Borreca, A., Puca, A.A., Stamler, J.S., Cecconi, F., Filomeni, G., 2018. S-nitrosylation drives cell senescence and aging in mammals by controlling mitochondrial dynamics and mitophagy. Proc. Natl. Acad. Sci. U.S.A. 115, 3388–3397.

Romero-Puertas, M.C., Laxa, M., Mattè, A., Zaninotto, F., Finkemeier, I., Jones, A.M.E., Perazzolli, M., Vandelle, E., Dietz, K.J., Delledonne, M., 2007. S-nitrosylation of peroxiredoxin II E promotes peroxynitrite-mediated tyrosine nitration. Plant Cell 19, 4120–4130.

Ryu, H., Cho, Y.G., 2015. Plant hormones in salt stress tolerance. J. Plant Biol. 58, 147–155.

Sami, F., Faizan, M., Faraz, A., Siddiqui, H., Yusuf, M., Hayat, S., 2018. Nitric oxide-mediated integrative alterations in plant metabolism to confer abiotic stress tolerance, NO crosstalk with phytohormones and NO-mediated post translational modifications in modulating diverse plant stress. Nitric Oxide-Biol. Ch. 73, 22–38.

Saxena, N., Won, J., Choi, S., Singh, A.K., Singh, I., 2018. S-nitrosoglutathione reductase (GSNOR) inhibitor as an immune modulator in experimental autoimmune encephalomyelitis. Free Radic. Biol. Med. 121, 57–68.

Sehrawat, A., Deswal, R., 2014. S-nitrosylation analysis in *Brassica juncea* apoplast highlights the importance of nitric oxide in cold-stress signaling. J. Proteome Res. 13, 2599–2619.

Seth, D., Hess, D.T., Hausladen, A., Wang, L., Wang, Y., Stamler, J.S., 2018. A multiplex enzymatic machinery for cellular protein S-nitrosylation. Mol. Cell 69, 451–464.

Smith, M.D., Licatalosi, D.D., Thompson, J.E., 2000. Co-association of cytochrome f catabolites and plastid-lipid-associated protein with chloroplast lipid particles. Plant Physiol. 124, 211–221.

Su, D., Shukla, A.K., Chen, B., Kim, J.S., Nakayasu, E., Qu, Y., Aryal, U., Weitz, K., Clauss, T.R.W., Monroe, M.E., et al., 2013. Quantitative site-specific reactivity profiling of S-nitrosylation in mouse skeletal muscle using cysteinyl peptide enrichment coupled with mass spectrometry. Free Radic. Biol. Med. 57, 68–78.

Tanou, G., Filippou, P., Belghazi, M., Job, D., Diamantidis, G., Fotopoulos, V., 2012. Oxidative and nitrosative-based signaling and associated post-translational modifications orchestrate the acclimation of citrus plants to salinity stress. Plant J. 72, 585–599.

Teige, M., Scheikl, E., Eulgem, T., Dóczi, R., Ichimura, K., Shinozaki, K., Dangl, J.L., Hirt, H., 2004. The MKK2 pathway mediates cold and salt stress signaling in Arabidopsis. Mol. Cell 15, 141–152.

Terrile, M.C., París, R., Calderón-Villalobos, L.I.A., Iglesias, M.J., Lamattina, L., Estelle, M., Casalongué, C.A., 2012. Nitric oxide influences auxin signaling through S-nitrosylation of the Arabidopsis TRANSPORT INHIBITOR RESPONSE 1 auxin receptor. Plant J. 70, 492–500.

Tichá, T., Lochman, J., Činčalová, L., Luhová, L., Petřivalský, M., 2017. Redox regulation of plant S-nitrosoglutathione reductase activity through post-translational modifications of cysteine residues. Biochem. Bioph. Res. Co. 494, 27–33.

Turkan, I., 2018. ROS and RNS: key signalling molecules in plants. J. Exp. Bot. 69, 3313–3315.

Wang, F., Jing, W., Zhang, W., 2014. The mitogen-activated protein kinase cascade

MKK1-MPK4 mediates salt signaling in rice. Plant Sci. 227, 181–189.
Wang, P., Du, Y., Hou, Y.J., Zhao, Y., Hsu, C.C., Yuan, F., Zhu, X., Tao, W.A., Song, C.P., Zhu, J.K., 2015. Nitric oxide negatively regulates abscisic acid signaling in guard cells by S-nitrosylation of OST1. Proc. Natl. Acad. Sci. U.S.A. 112, 613–618.
Wojdyla, K., Williamson, J., Roepstorff, P., Rogowska-Wrzesinska, A., 2015. The SNO/SOH TMT strategy for combinatorial analysis of reversible cysteine oxidations. J. Proteomics 113, 415–434.
Wolhuter, K., Whitwell, H.J., Switzer, C.H., Burgoyne, J.R., Timms, J.F., Eaton, P., 2018. Evidence against stable protein S-nitrosylation as a widespread mechanism of post-translational regulation. Mol. Cell 69, 438–450.
Yang, H., Mu, J., Chen, L., Feng, J., Hu, J., Li, L., Zhou, J.M., Zuo, J., 2015. S-nitrosylation positively regulates ascorbate peroxidase activity during plant stress responses. Plant Physiol. 167, 1604–1615.
Yun, B.W., Feechan, A., Yin, M., Saidi, N.B.B., Bihan, T.L., Yu, M., Moore, J.W., Kang, J.G., Kwon, E., Spoel, S.H., Pallas, J.A., Loake, G.J., 2011. S-nitrosylation of NADPH oxidase regulates cell death in plant immunity. Nature 478, 264–268.
Zaffagnini, M., Bedhomme, M., Marchand, C.H., Morisse, S., Trost, P., Lemaire, S.D., 2012. Redox regulation in photosynthetic organisms: focus on glutathionylation. Antioxidants Redox Signal. 16, 567–586.
Zhan, N., Wang, C., Chen, L., Yang, H., Feng, J., Gong, X., Ren, B., Wu, R., Mu, J., Li, Y., Liu, Z., Zhou, Y., Peng, J., Wang, K., Huang, X., Xiao, S., Zuo, J., 2018. S-Nitrosylation targets GSNO reductase for selective autophagy during hypoxia responses in plants. Mol. Cell 71, 142–154.
Zhang, A., Jiang, M., Zhang, J., Ding, H., Xu, S., Hu, X., Tan, M., 2007. Nitric oxide induced by hydrogen peroxide mediates abscisic acid-induced activation of the mitogen-activated protein kinase cascade involved in antioxidant defense in maize leaves. New Phytol. 175, 36–50.
Zhou, H., Finkemeier, I., Guan, W., Tossounian, M.A., Wei, B., Young, D., Huang, J., Messens, J., Yang, X., Zhu, J., Wilson, M.H., Shen, W., Xie, Y., Foyer, C.H., 2018. Oxidative stress-triggered interactions between the succinyl- and acetyl-proteomes of rice leaves. Plant Cell Environ. 41, 1139–1153.